Retinal microvasculature alteration in central serous chorioretinopathy

LI YU[1], YI SHAO[2], YONG CHAI[1], LIN-HONG YE[2], QI-CHEN YANG[3], LEI YE[2], QING YUAN[2], NAN JIANG[3] and JING-LIN YI[1]

[1]Department of Opthalmology, Affiliated Eye Hospital of Nanchang University; [2]Department of Ophthalmology, The First Affiliated Hospital of Nanchang University, Nanchang, Jiangxi 330006; [3]Eye Institute of Xiamen University, Fujian Provincial Key Laboratory of Ophthalmology and Visual Science, Xiamen, Fujian 361102, P.R. China

Received May 6, 2017; Accepted November 14, 2017

DOI: 10.3892/mmr.2017.8126

Abstract. The aim of the present study was to investigate the changes of retinal microvascular network in patients with central serous chorioretinopathy (CSCR). A total of fifteen patients (right eye) with CSCR and 15 normal controls (right eye) were recruited. We used optical coherence tomography angiography to scan 6x6 mm macular retinal blood flow images with the application of a series of customized image segmentation processing program software to obtain microvascular and macrovascular density, and compared the superficial microvascular (SMIR), superficial macrovascular ring (SMAR) and the superficial total microvascular (STMI) density between CSCR patients and control group. Using the annular partition (C1-C6) and quadrant partition methods on the macular, we compared the retinal vessel density changes. We also performed ROC analysis of superficial retinal microvessel density in CSCR retina to investigate the relationship between the microvascular density, the foveal thickness and visual acuity. The density of STMI and SMIR decreased in macular area in the patients with CSCR compared to the normal controls ($P<0.05$), while the density of SMAR did not change significantly. We found no significant difference in the density of SMIR with the quadrant partition method, whereas the annular partition method showed significantly decreased SMIR density only in the C1 region in patients with CSCR ($P<0.05$), with no significant difference observed in C2-C6 regions. The density of SMIR had the highest differentiation power in the CSCR group, whereas the density of SC1 ring had the lowest differentiation power by the annular method. The largest area under the ROC curves was 0.77. The correlation index of the SMIR density and visual acuity was -0.544, whereas macular thickness and visual acuity was -0.644 in the CSCR group. The density of STMI and SMIR were decreased in patients with CSCR, which might provide further understanding of the pathogenesis of CSCR.

Correspondence to: Professor Jing-Lin Yi, Department of Opthalmology, Affiliated Eye Hospital of Nanchang University, 463 Bayi Avenue, Donghu, Nanchang, Jiangxi 330006, P.R. China
E-mail: freebee99@163.com

Key words: microvasculature, optical coherence tomography angiography, fractal analysis, central serous chorioretinopathy

Introduction

Central serous chorioretinopathy (CSCR) is characterized by serous detachment of posterior pole retinal sensory layer from the pigment epithelium, which results in the leakage of retinal pigment epithelium, with or without pigment epithelium detachment (1). Fundus angiography is an important method for the diagnosis of CSCR. Previous studies using indocyanine green angiography (ICGA) showed that CSCR is mainly associated with choroid perfusion abnormalities, while the retinal pigment epithelium (RPE) lesions and accumulation of subretinal fluid are secondary changes (2), suggesting that CSCR may be caused by choroid microvascular lesions. It is well known that CSCR is a self-limiting disease, and the majority of patients generally self heal within 3-6 months, but chronic and recurrent occurrence can eventually lead to permanent loss of vision (3). However, the exact pathogenesis of CSCR remains unclear. As a result, it is important to discover a method to determine whether patients with early stage can self heal, and provide guidelines for early intervention to avoid permanent loss of vision caused by CSCR for patients who can not self heal.

Optical coherence tomography (OCT) plays a very important role in the diagnosis of CSCR. The fundus image OCT can evaluate the subretinal fluid volume and location of RPE lesion, and provide information for the diagnosis and treatment of CSCR. However, it does not provide clear clues for choroidal and retinal vasculature (4). In recent years, the optical coherence tomography angiography (OCTA) has successfully solved this problem. It is a new noninvasive imaging technique compared with the traditional OCT. The most prominent advantage of OCTA system is the application of the SSADA algorithm (5) and En-face scanning. The SSADA algorithm can reduce the artifacts and noise to a certain extent, and improve the signal to noise ratio. The application of En-face can obtain three-dimensional image data, displaying all aspects of information, such as the retinal

nerve fiber layer, RPE, and choroid. In addition, OCTA is not affected over time, since it is a non-invasive method without injection of contrast agent (5). OCTA provides a detailed view of the retinal blood vessels, and can accurately describe retinal microvascular abnormalities and vascular occlusion. It can also help to quantify vascular damage.

Combined with previous studies, it has been shown that the pathological changes of CSCR are mainly choroidal microvascular abnormalities, and whether there is a change in the microvessels in the macular region remains unexplored. In this study, OCTA was used to quantify the retinal microvascular density, and to explore the changes of retinal microvascular network in patients with CSCR.

Materials and methods

Research subjects. To ensure the maximum comparability between the experimental group and the control group, we conducted a prospective randomized controlled study. To minimize the effects of non-experimental factors, such as age and course of disease, we recruited 15 CSCR patients (all right eye) with symptoms duration less than 1 months according to the principle of minimum distribution imbalance index from the Affiliated Eye Hospital and First Affiliated Hospital of Nanchang University from 2016 to 2017, and 15 age and gender matched healthy participants (all right eye) as control group. The subjects completed a comprehensive examination of the ocular surface and OCTA. The clinical manifestations of CSCR included decreased visual acuity, blurred vision, visual distortion, light shadow occlusion, dim vision, dark landscape and so on.

Recruitment criteria. For all patients, diagnosis was based on the best-corrected visual acuity (BCVA), routine eye examination, and fundus fluorescein angiography (FFA) examination (6). In accordance with CSCR diagnostic criteria, clinical presentation of the disease included: i) clinical manifestations of visual impairment, floating shadows or central scotoma (blind spot), visual darkening, discoloration, deformation, narrowing; ii) FFA examination showing macular edema or discoid anti-halo, with or without yellow/white punctiform exudation or old exudative spots; iii) FFA examination showing either the typical or atypical punctate pigment epithelial leakage on the posterior pole and smoke-like or ink-like stains on the macular area.

Exclusion criteria. The exclusion criteria were: i) eyelid disease and other ocular surface diseases and intraocular diseases that were not cured; ii) eye surgery within six months; iii) rheumatoid arthritis, systemic lupus erythematosus, Sjogren syndrome and other systemic autoimmune disease; iv) long period administration of anti hypertension and anti depressants drugs; v) pregnant or lactating patients.

Ethical considerations. The present study was conducted in accordance with the principles of the declaration of Helsinki, according to the requirements of the two hospitals' ethics committee. A detailed explanation of the method and content of the study was given to each patient, and the consent was signed by the patient.

OCTA. OCTA image was taken using the RTVue Avanti XR system (Optovue, Fremont, CA, USA). This device has recently been introduced into clinical practice for simultaneous visualization of retinal cross sections and blood vessels. The instrument scanned at 70000 A-per second, including a super light emitting diode, with a central wavelength of 840 nm and a bandwidth of 45 nm (6). It provided an axial resolution of 5 μm within the tissue, and the retinal plane spot diameter was 22 μm (horizontal resolution). A series of B scans were obtained over a 6x6 mm area focused on the concave obtained choroidal OCTA images (Fig. 1 A-C). Each B scan contained 216 A-scans (along the X axis) and five consecutive B scans were captured at each of the 216 locations (along the Y axis). With a speed of 270 frames per second, a total of 1080 B scans (216 y-positions x 5 positions) were obtained. 6x6 mm OCTA image acquisition was created by a set of four volume scans, including a total of two horizontal and a set of two vertical gratings (a total of 933 120 A-scans). Kraus *et al* (7) has shown that it is based on the use of an algorithm for orthogonal scan alignment to correct motion artifacts.

The system used RTVue XR to create the OCTA images (8). Simply put, it is an algorithm for computing the correlation of the amplitude of a series of spots from the same pixel at the same location. The correlation in the speckle amplitude can be related to the cardiac cycle from the motion of the blood vessels or the pulsating motion of the whole retina. In contrast to the OCT beam moving toward the vertical moving blood cells, the eye pulsations occur along the axial direction. The resolution of the asymmetric OCT system, in which the axial resolution is typically 3 to 5 times higher than the lateral resolution, results in higher sensitivity to tissue motion than the axial resolution. In order to improve the signal-to-noise ratio of detection, the RTVue XR Avanti system utilizes four different frequency bandwidths of OCT to reduce the noise of the axial motion. This modification creates four voxel data sets with the same resolution (20x20x20 M instead of 20x20x5 M in full spectrum light source). Decorrelation of each pixel is performed at each frequency band to calculate the average increased traffic signal. High-resolution correlation is the value of low correlated speckle amplitude derived from blood flow, tissue motion and background noise. Decorrelation signal reduces the outliers (too high decorrelation) and the zero correlation value of the arbitrarily assigned voxel backscatter amplitude is lower than the threshold value (8). Because of the influence of liquid in the macular area of CSCR patient, the deep layer intra-retinal of OCTA image was not clear.

Statistical analysis. All data were analyzed with a statistical package (Statistica, v7.1; StatSoft, Inc, Tulsa, OK, USA), MedCalc software (v10; MedCalc Software, Mariakerke, Belgium). Continuous variables were presented as mean ± standard deviation (SD). One-way analysis of variance (ANOVA) was used to analyze superficial vessel density in sectors between groups. Least significant difference post hoc tests were used to assess the pairwise difference. $P<0.05$ was considered to indicate a statistically significant difference. The G *Power 3.0.10 software was used for the power calculation, which has statistical power (n=15) in the present study. The receiver operating characteristic (ROC) curve was plotted for the proposed superficial retinal vessel density in differentiating between healthy and diseased subjects.

Results

Patients before treatment. Study population statistics are shown in Table I. CSCR group (n=15) and control group (n=15) were not statistically significant (P>0.05) in gender, age, axial length, diastolic blood pressure, systolic blood pressure, heart rate, but there was significant difference in macular edema diameter (P<0.05).

Macular vascular density. Firstly, we compared the density of superficial microvascular (SMIR), superficial macrovascular ring (SMAR) and superficial total microvascular (STMI) in both groups. We found that compared with the control group, the density of SMIR and STMI was significantly decreased in CSCR patients (P<0.05), while the density of SMAR was not significantly changed (Fig. 2A). Secondly, we used the hemispheric partition (Fig. 1C and F) and Early Treatment Diabetic Retinopathy Study (ETDRS) method (Fig. 1B and E) to compare the density of SMIR, and we found that the two partition methods were not significant different (P>0.05, Fig. 2B and C), indicating there was no quadrant changes in the density of SMIR. Lastly, we used the ring partition method (Fig. 1A and D) to compare the microvascular density. The results showed that there was a significant decrease in the density of blood vessels in C1 partition (P<0.05, Fig. 2D). There was also a decreasing trend in other partitions, but not statistically significant (P>0.05).

ROC analysis of superficial retinal microvessel density. The vessel density of the superficial retina provided by OCTA had the best sensitivity-specificity pairs for differentiating CSCR from controls. The density of SMIR had the highest positive likelihood ratios in the CSCR group, whereas the C1 density of the superficial retina had the lowest negative likelihood ratio by the annular method. The largest area under the ROC curves was 0.77 (Fig. 3).

Correlation between macular blood vessel density, foveal thickness and visual acuity. We analyzed the correlation between SMIR, SMAR, STMI and macular thickness (Fig. 4). There was no correlation between the density of SMAR, STMI and visual acuity in the superficial retinal layer (P>0.05, data not shown). The correlation index of the SMIR density and visual acuity in the CSCR group was -0.544 (Fig. 4A). These results suggested that reduced SMIR density in the macular area could affect the visual acuity. The correlation index of macular thickness and visual acuity in the CSCR group was -0.644 (P<0.05) (Fig. 4B), indicating that the changes in the macular thickness would have an affect on visual acuity.

Discussion

CSCR usually affects young and middle-aged people. Most patients can self heal, but chronic CSCR is persistent, prone to recurring, and has long duration. It can also cause irreversible damage to the patient's vision (9). The current studies mainly believe that the original CSCR lesions occur in the choroid, leakage of RPE blood retinal barrier of blood vessels, leading to the occurrence of CSCR (10). This is the first study showing reduced retinal superficial microvessel density in the macular

Table I. Baseline characteristics of patients in the study.

Variables	HCs	CSCR
Age (range, years)	49±6	48±8
Sex ratio, male:female	5:10	7:8
RE (range, diopters)	1.00±0.90	5.00±1.00
	0~-2.75	-3~-5.75
AL (mm)	23.54	24.01
SBP (mmHg)	119±8	117±12
DBP (mmHg)	78±9	80±11
HR	78±12	76±14
Macular volume	0	1.18±0.31

Results are presented as the mean ± standard deviation. AL, axial length; CSCR, central serous chorioretinopathy; DBP, diastolic blood pressure; HR, heart rate; RE, refraction diopter; SBP, Systolic blood pressure; and SD, Standard deviation. *P<0.05 HCs vs. CSCR.

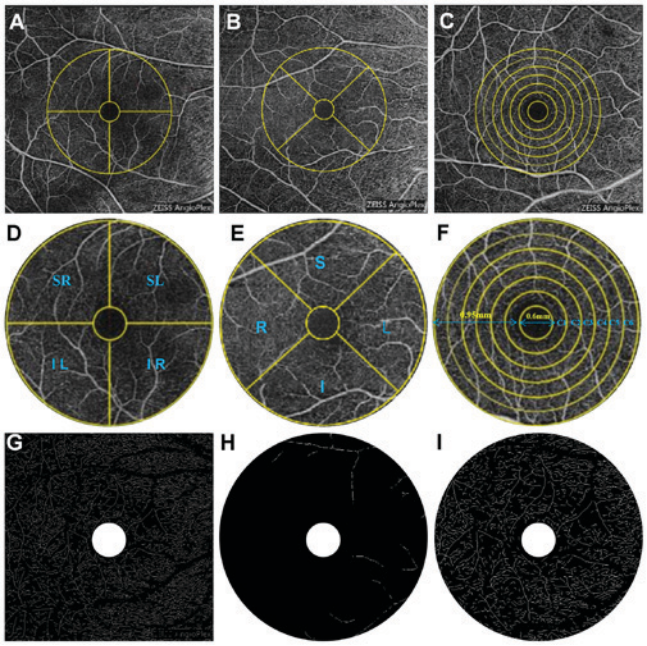

Figure 1. OCTA scans of the 6x6 mm shallow image of the macular region of the retina. (A) Hemispheric partition method: The image is divided into 4 quadrants of vertical and horizontal regions, followed by R, S, L and I. (B, E) Early Treatment Diabetic Retinopathy Study ring area is divided into 4 quadrants by the diagonal of the two quadrants. (C) The algorithm searches from the center to the periphery of the macular 6x6 mm image with intensity gradient detection software to identify the foveal avascular zone center (FAZ). (D, E) Customized segmentation image processing program divided images into (D) SR, SL, IL and IR and (E) S, L, and R quadrants, and included a series of actions such as inverting, balancing, and removal of the background noise and non-vessel structure to create a binary image, and retained the individual microvascular skeletonization image with diameter larger than 25 mm and large vessels remained after the removal of small vessels. (F) After removal of the avascular zone (0.6 mm diameter of the fovea), a circular region of 0.6 to 2.5 mm in diameter is defined as the ring with bandwidth of 0.95 mm. The annular region is divided into 6 thin rings with a bandwidth of 0.16 mm. (G) The skeletonized image of superficial total microvascular: 6x6 mm macular area. (H) The skeletonized image of superficial macrovessel ring: 3 mm macular ring area. (I) The skeletonized image of superficial microvessel ring: 3 mm macular ring area. I, inferior; IL, inferior left; IR, inferior right; L, left; R, right; S, superior; SC, superficial central annuli; SL, superior left; SMAR, superficial macrovascular ring; SMIR, superficial microvessel ring; SR, superior right; STMI, superficial total microvascular.

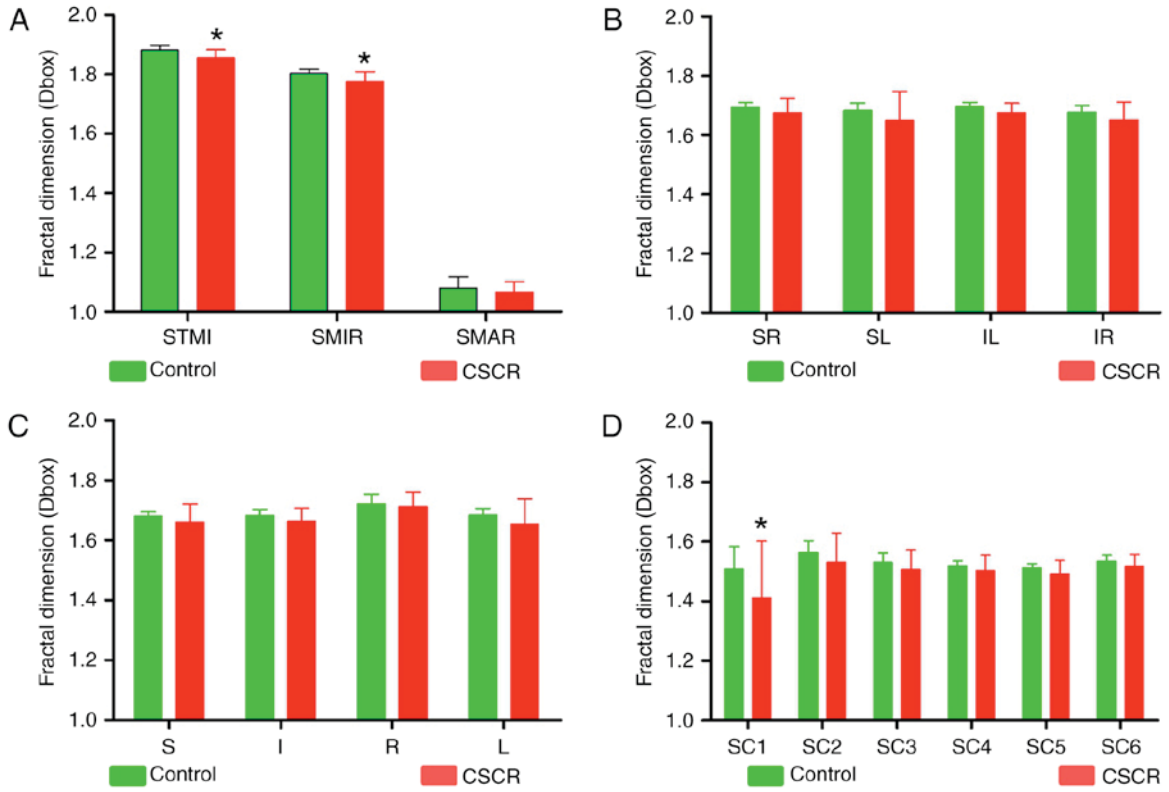

Figure 2. Comparisons of macula retinal vessel density (D box) between CSCR and control subjects in the superficial layer. (A) Compared with the control group, there was a significant difference in the density of superficial total microvascular and superficial microvascular ring in macular region of CSCR patients (P<0.05). (B) The density of superficial microvessels in the CSCR group was not significantly changed compared to the control group for all quadrantal methods like the (B) Hemispheric partition method and (C) ETDRS method about the superficial retinal layers (all P>0.05). (D) In the CSCR group, except for the Cl partition of the superior retinal layer (P<0.05), the microvessel density was not significantly changed compared to the control group for all quadrantal zones of the superficial retinal layers (all P>0.05). *P<0.05 in control vs. CSCR. I, inferior; IL, inferior left; IR, inferior right; L, left; R, right; S, superior; SC, superficial central annuli; SL, superior left; SMAR, superficial macrovascular ring; SMIR, superficial microvascular ring; SR, superior right; STMI, superficial total microvascular' CSCR, central serous chorioretinopathy.

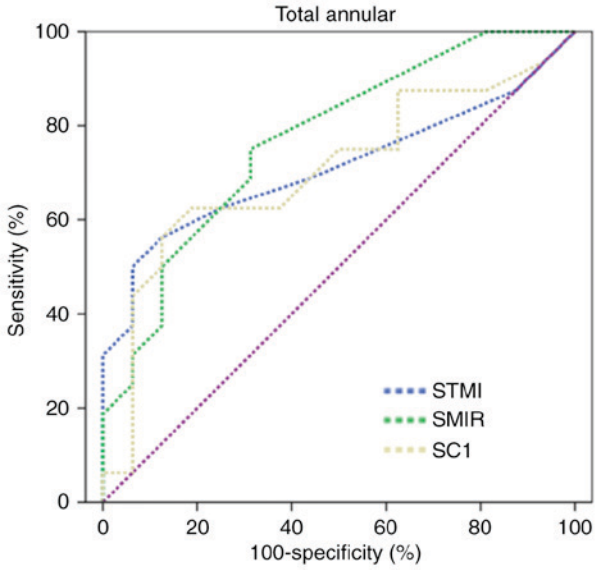

Figure 3. ROC analysis of annular, quadrantal and sectorial microvessel density. Representation of ROC curves obtained with the density of the superficial vessel in the CSCR provided by the optical coherence tomography angiography device. The largest areas under the ROC curves for the density of SMIR were 0.77 (95% CI=0.61-0.94), and the lowest areas under the ROC curves for SC1 density of the superficial retina were 0.71 (95% CI=0.52-0.89). ROC, Receiver operating characteristic curves; SC1, superficial central annuli 1; SMAR, superficial macrovascular ring; SMIR, superficial microvascular ring; STMI, superficial total microvascular.

regions of the CSCR patients, providing evidence for a more comprehensive understanding of CSCR.

In patients with CSCR, there are usually one or a few small areas of serous retinal pigment epithelial detachment in the macular region. Prunte *et al* found that choroidal capillary lobules and their venous blood retention were related to the pigment epithelium detachment and leakage (11). ICGA found that CSC patients had not only changes of RPE leakage, but also delayed perfusion of the choroid, dilation of choroidal capillary and vein, increased choroidal vascular permeability, pigment epithelial detachment (PED) and recessive pigment epithelial detachment (12). According to the pathogenesis of CSCR proposed by Caccavale: Many factors lead to vasoconstriction and capillary congestion, causing decreased vascular bed, increased resistance to blood flow and blood viscosity, and further vascular bed hypoperfusion and increased cavity pressure. These result in increased intraluminal pressure in the stroma of serum and small molecule leakage, further blocking the blood vessels, eventually increasing permeability of the choroid capillary. The exudation by RPE leaks into the subretinal space, causing RPE decompensation and detachment, and finally the formation of CSCR (13). We observed that total macular retinal microvessel density and microvessel density was significantly reduced in CSCR patients compared with the control group, suggesting that CSCR induces changes of

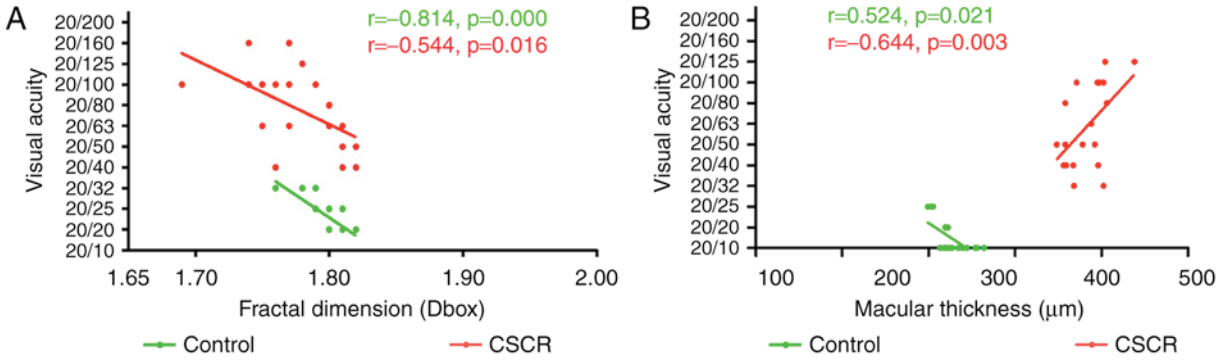

Figure 4. Correlation analyses between retinal vessel density, macular fovea thickness and visual acuity in superficial retinal layer. (A) The density of SMIR (D box) was correlated with visual acuity (r=-0.544, P=0.016). (B) Correlation between macular thickness and visual acuity (r=-0.644, P=0.003). CSCR, central serous chorioretinopathy; MFT, macular fovea thickness.

choroidal capillary, and may also cause the change of retinal capillaries, but the mechanism needs further study.

The present study showed that the density of SMIR in the annular C1 partition was significantly reduced in the CSCR patients, and there was no statistically significance in the C2-C6 partitions, suggesting that the macular retinal vascular density reduction in CSCR patients might be mainly concentrated near central fovea region. However, there was no significant difference in the changes of macular retinal blood vessel density in patients with CSCR, indicating that there was no correlation between macular area and vascular density in patients with CSCR. This might be related to serous detachment caused by CSCR.

There are two main retinal blood supply systems. The outer retina is mainly supplied through the choroidal blood circulation, and retinal blood circulation provides supply and nutrition for the inner retina. The blood choriocapillary layer nourishes retinal neuroepithelial layer (layer of retinal neurons to the outer plexiform layer) of the optic nerve, and usually is the only source of nutrition for fovea (14). The retinal blood flow and choroidal blood circulation changes will directly affect the vision of patients. We found that the total macular retinal microvessel density and visual acuity had significant correlation, and reduction of the macular retinal microvascular density did not have effects on visual acuity. That might be because of the difference in disease stage, which needs further investigation with a larger sample size.

OCTA plays an important role in the diagnosis of CSCR, because it can not only be used to observe the retinal neuroepithelial layer morphology and the changes of RPE, but also can be used to track the changes of the disease, such as subretinal fluid changes (15). CSCR induces retinal serous detachment, and causes decreased visual acuity, central scotoma, metamorphopsia, dyschromatopsia, decreased visual size and visual contrast sensitivity (9,16). And there is a positive correlation between the serous detachment height and vision quality. As a result, OCT tracks disease condition mainly based on observation of changes of retinal thickness and we found that changes of the central macular thickness had a significant influence on visual acuity, which is consistent with previous studies. In this study, OCTA showed accumulation of subretinal fluid, RPE layer defects, and a typical dye leakage from the choroid into the subretinal space in CSCR patients. In most cases, the prognosis was good, with spontaneous regression and good visual acuity. However, some patients might suffer from vision impairment, which might be due to a recurrence of the disease or a secondary angiogenesis (17). Filho *et al* reported that OCTA had higher sensitivity and specificity compared with FAA detection of chronic CSCR in CNV (18).

The reduction of retinal vascular network in CSCR patients is regarded as an indicator of the progression of macular degeneration, which is usually manifested as retinal vascular disease. Changes of visual acuity occur in the early onset of macular degeneration. CSCR manifested in OCTA as granular inhomogeneous high reflection with small pieces of dark area at the choriocapillary level, and 70% of the patients with high reflection region matched with the high permeability area as seen with ICGA. RPE CNV could be visualized by OCTA in 21% patients with double signs of CSCR. OCTA can be used in the follow-up of patients with CSCR, and can better show the choroidal ischemia after PDT. The development of OCTA can promote our understanding of the pathogenesis of CSCR (19).

Carlo *et al* (20) used OCTA to observe the irregular shedding of RPE in CSCR patients, and found that CSCR patients showed increased possibility of angiogenesis in irregular vascular RPE shedding, which is helpful for the treatment. Shozo *et al* (21) found that inflammation at the high level of choroid reflex in the acute phase of CSCR was associated with edema. The high reflecting area outside the choroid is the expansion of the vascular lumen of the great vessels, regardless of the onset of CSCR. Feucht *et al* (22) found no changes in the blood flow parameters associated with acute CSCR leakage in the OCTA images of the superficial and deep retinal nerve plexus, the outer retina, and the choroidal capillaries. But the changes of intraocular choroidal blood flow could be quantified. Studies (23) have shown that retinal abnormalities, especially lattice degeneration, are often seen in patients with CSCR. Therefore, the authors suggested that CSCR patients should be regularly examined for the retinal health, including the assessment of the peripheral retina.

There are some inadequacies in the present study. For example, we only observed the density of SMIR, SMAR and SC1 changes in the macular of patients with CSCR. Whether it is consistent with choroidal microvascular changes, or happens before or after the choroidal microvascular changes, and whether it can be used as an early indicator of self-healing remain to be further explored.

Acknowledgements

This work was supported by grants from the National Natural Science Foundation of China [NSFC no. 81160118 (Yi Sh), 81460092 (Yi Sh) and 81660152 (Yi Sh)].

References

1. Kang S, Park YG, Kim JR, Seifert E, Theisen-Kunde D, Brinkmann R and Roh YJ: Selective retina therapy in patients with chronic central serous chorioretinopathy: A pilot study. Medicine (Baltimore) 95: e2524, 2016.
2. Guyer DR, Yannuzzi LA, Slakter JS, Sorenson JA, Ho A and Orlock D: Digital indocyanine green videoangiography of central serous chorioretinopathy. Arch Ophthalmol 112: 1057-1062, 1994.
3. Klatt C, Saeger M, Oppermann T, Pörksen E, Treumer F, Hillenkamp J, Fritzer E, Brinkmann R, Birngruber R and Roider J: Selective retina therapy for acute central serous chorioretinopathy. Br J Ophthalmol 95: 83-88, 2011.
4. Adhi M and Duker JS: Optical coherence tomography-current and future applications. Curr Opin Ophthalmol 24: 213-221, 2013.
5. Miwa Y, Murakami T, Suzuma K, Uji A, Yoshitake S, Fujimoto M, Yoshitake T, Tamura Y and Yoshimura N: Relationship between functional and structural changes in diabetic vessels in optical coherence tomography angiography. Sci Rep 6: 29064, 2016.
6. Spaide RF, Klancnik JM jr and Cooney MJ: Retinal vascular layers imaged by fluorescein angiography and optical coherence tomography angiography. JAMA Ophthalmol 133: 45-50, 2015.
7. Kraus MF, Potsaid B, Mayer MA, Bock R, Baumann B, Liu JJ, Hornegger J and Fujimoto JG: Motion correction in optical coherence tomography volumes on a per A-scan basis using orthogonal scan patterns. Biomed Opt Expr 3: 1182-1199, 2012.
8. Jia Y, Tan O, Tokayer J, Potsaid B, Wang Y, Liu JJ, Kraus MF, Subhash H, Fujimoto JG, Hornegger J and Huang D: Split-spectrum amplitude decorrelation angiography with optical coherence tomography. Opt Express 20: 4710-4725, 2012.
9. Wang M, Munch IC, Hasler PW, Prünte C and Larsen M: Central serous chorioretinopathy. Acta Ophthalmol 86: 126-145, 2008.
10. Kishi S, Yoshida O, Matsuoka R and Kojima Y: Serous retinal detachment in patients under systemic corticosteroid treatment. Japanese J ophthalmol 45: 640-647, 2001.
11. Prunte C and Flammer J: Choroidal capillary and venous congestion in central serous chorioretinopathy. Am J Ophthalmol 121: 26-34, 1996.
12. Piccolino FC and Borgia L: Central serous chorioretinopathy and indocyanine green angiography. Retina 14: 231-242, 1994.
13. Caccavale A, Romanazzi F, Imparato M, Negri A, Morano A and Ferentini F: Central serous chorioretinopathy: A pathogenetic model. Clin Ophthalmol 5: 239-243, 2011.
14. Cunha-Vaz J, Bernardes R and Lobo C: Blood-retinal barrier. Eur J Ophthalmol 21: S3-S9, 2011.
15. Montero JA and Ruiz-Moreno JM: Optical coherence tomography characterisation of idiopathic central serous chorioretinopathy. Br J Ophthalmol 89: 562-564, 2005.
16. Daruich A, Matet A and Behar-Cohen F: Central serous chorioretinopathy. Dev Ophthalmol 58: 27-38, 2017.
17. Chalam KV and Sambhav K: Optical coherence tomography angiography in retinal diseases. J Ophthalmic Vis Res 11: 84-92, 2016.
18. Bonini Filho MA, de Carlo TE, Ferrara D, Adhi M, Baumal CR, Witkin AJ, Reichel E, Duker JS and Waheed NK: Association of choroidal neovascularization and central serous chorioretinopathy with optical coherence tomography angiography. JAMA Ophthalmol 133: 899-906, 2015.
19. Bousquet E, Bonnin S, Mrejen S, Krivosic V, Tadayoni R and Gaudric A: Optical coherence tomography angiography of flat irregular pigment epithelium detachment in central serous chorioretinopathy. Retina, 2017.
20. de Carlo TE, Rosenblatt A, Goldstein M, Baumal CR, Loewenstein A and Duker JS: Vascularization of irregular retinal pigment epithelial detachments in chronic central serous chorioretinopathy evaluated with OCT angiography. Ophthalmic Surg Lasers Imaging Retina 47: 128-133, 2016.
21. Sonoda S, Sakamoto T, Kuroiwa N, Arimura N, Kawano H, Yoshihara N, Yamashita T, Uchino E, Kinoshita T and Mitamura Y: Structural changes of inner and outer choroid in central serous chorioretinopathy determined by optical coherence tomography. PLoS One 11: e0157190, 2016.
22. Feucht N, Maier M, Lohmann CP and Reznicek L: OCT angiography findings in acute central serous chorioretinopathy. Ophthalmic Surg Laser Imaging Retina 47: 322-327, 2016.
23. Oztas Z, Akkin C, Ismayilova N, Nalcaci S and Afrashi F: The importance of the peripheral retina in patients with central serous chorioretinopathy. Retina, 2017.